Research Papers

GREENSUSMATER

Greensusmater
Vol. 1, No. 1, March 2024
https://doi.org/10.62755/greensusmater.2024.1.1.25-31

Check for updates

Degradation of air pollutants from waste burning using photocatalyst TiO_2 With $Co(NO_3)_2$ doped under ultraviolet irradiation

Kamila Munna[1,†] Rizky Aflaha[2,†] Chotimah[2,]

[1] *Department of Physics, Faculty of Mathematics and Natural Sciences, Institut Teknologi Bandung, Jalan Ganesha 10, Bandung 40132, Indonesia*
[2] *Department of Physics, Faculty of Mathematics and Natural Sciences, Universitas Gadjah Mada, Sekip Utara, BLS 21, Yogyakarta 55281, Indonesia*
[†]These authors contributed equally to this work.

Corresponding author: chotimah_w@ugm.ac.id

ARTICLE HISTORY: Received: March 4, 2024 | Revised: March 11, 2024 | Accepted: March 13, 2024

ABSTRACT

Air pollutants, such as carbon dioxide (CO_2), hydrogen cyanide (HCN), and methane (CH_4), can harm the respiratory organs of humans and cause several diseases. This study successfully utilized a photocatalyst from TiO_2 with $Co(NO_3)$ doped to degrade these air pollutants from waste burning. The photocatalyst layer was produced by dissolving TiO_2 and $Co(NO_3)_2$ in distilled water, and then the solution was coated on a mica surface using a spray coating method. The coated mica was then dried in an oven. The crystallite structure of $TiO_2/Co(NO_3)_2$ was analyzed by X-ray diffraction. The obtained crystallite size was (15.38 ± 0.03) nm with lattice parameters a and c were (3.8 ± 0.3) Å and (9.3 ± 0.3) Å, respectively, which shows that it is an anatase phase. The band gap energy was measured by diffuse reflectance UV-visible spectroscopy and analyzed using Tauc's plot method. The measured band gap energy of the photocatalyst was 2.81 eV, which can be easily activated by ultraviolet (UV) light. The photocatalyst sheets successfully degraded air pollutants from waste burning, including 53.139% CO_2 for 4 hours, 100% HCN for 10 minutes, and 72.381% CH_4 for 40 minutes. Therefore, the fabricated photocatalyst in this study can potentially be an alternative to degrading air pollutants, especially CO_2, HCN, and CH_4.

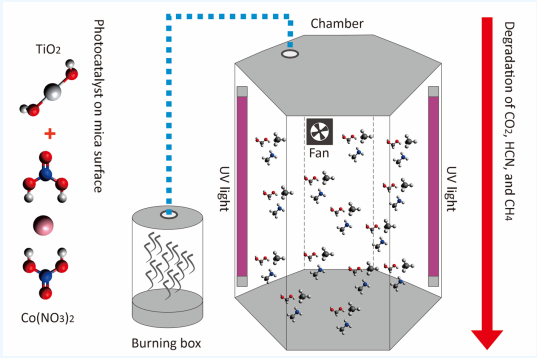

Keywords: *Photocatalyst, TiO_2, $Co(NO_3)_2$, Air Pollutants, UV Light*

1. INTRODUCTION

Fresh air is a very important element for living things. However, the fresh air issue has recently taken center stage because of air pollution. Air pollution is a mixture of gases and particles produced by many sources, such as the smoke of cigarettes, vehicles, industry, agriculture, combustion, and natural sources [1, 2, 3]. Several gases widely known as air pollutants include SO_2, NOx, NH_3, and CO, as well as greenhouse gases such as CO_2, CH_4, and N_2O [4, 5]. These pollutants pose significant risks to human health, particularly when they infiltrate indoor spaces through air vents. Confined within walls and roofs, these gases are impeded from dispersing naturally with the wind. Consequently, occupants inhale the pollution readily, leading to many health issues and compromising the overall comfort of the indoor environment [6].

Researchers have made various efforts to reduce air pollutants. Photocatalysis, an environmentally friendly and sustainable technique, holds great promise for degrading these pollutants [7, 8, 9]. Photocatalyst is a catalytic process whose success depends on light absorption capability, active site density, redox capacity, and the rate of light-triggered electron-hole recombination [10]. Titanium dioxide (TiO_2) is one of the most excellent and popular semiconductor photocatalysts, with good photosensitivity and chemical stability, non-toxicity, and low cost [11, 12]. TiO_2 has a crystallite size of 19.82 nm [13]. This crystal is divided into three polymorphic forms: rutile, anatase, and brookite [14, 15]. TiO_2 is used exclusively as a white pigment and has been widely used as a base material for producing sunscreen, photocatalysts, and solar cells [16]. However, this photocatalyst has limited optical and electronic properties that are active only when exposed to UV light [17], which is only ± 5% of solar energy [18]. The band gap energy on TiO_2 is about 3.23 eV [19].

Modifying the surface of TiO_2 by incorporating other materials is recognized as an effective technique to enhance the efficiency of sunlight utilization and broaden its photocatalytic activity [13]. Doping of metal ions (such as Fe, Co, Ag, Ni) and non-metallic elements (such as C, N, F, S) or carbon-containing materials (such as carbon nanotubes, flora, and graphene oxide) can improve the photocatalytic properties of TiO_2 [13, 17]. Among these materials, Co can effectively enhance the photocatalytic activity of TiO_2 [20]. When Co is introduced into the TiO_2 material, it acts as an impurity within the conduction band, leading to an electronic transition, namely the band gap transition from the valence band consisting of O 2p orbitals to the Co 3d and Ti 3d conduction bands. This intensity indicates that TiO_2/Co has good photocatalytic activity. After electron excitation, the pho-

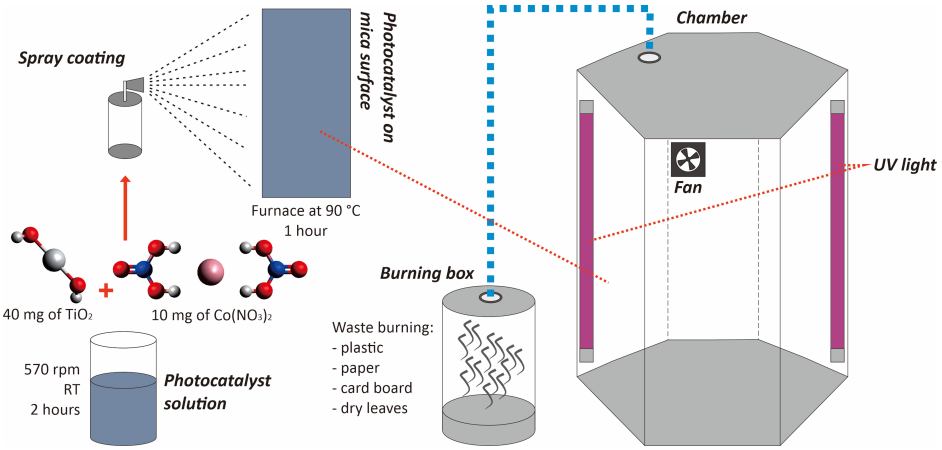

Figure 1. The chamber of photocatalyst test. The smoke sample flows from the burning box to the chamber. UV lamps are used as light sources.

togenerated electrons are reserved in the conduction band, which are further transferred to the surface of catalyst particles to be captured by O_2 molecules adsorbed on the surface. The photogenerated holes in the valence band are trapped by hydroxyl molecules and water as active radicals to oxidize organic compounds [20].

Hosseini et al. found that a fabricated photocatalytic mixed matrix membrane containing Co and TiO_2 nanoparticles was suitable for the photocatalytic separation of 2,4-dichlorophenol [13]. Khaki et al. also researched Co and TiO_2, which resulted in the bandgap energy of the transition metal Co-doped with TiO_2 being lower than that of TiO_2, which is 2.96 eV [17]. In addition to its utilization in liquid samples, TiO_2 can also be used in gas samples. Mamaghani et al. carried out hydrothermal/solvothermal synthesis and processing of TiO_2 as an effective photocatalyst for the degradation of air pollutants [21]. Therefore, research on photocatalysts for the degradation of air pollutants is possible.

In this study, TiO_2 with a Co-doped photocatalyst was fabricated. To assess the impact of Co doping on the crystallite structure of TiO_2, X-ray diffraction (XRD) patterns were conducted. Additionally, to confirm that Co doping reduces the band gap energy of TiO_2, testing was performed using diffuse reflection UV-visible (DR UV-Vis) spectroscopy. The photocatalyst was tested to degrade the air pollutants, namely CO_2, HCN, and CH_4, from waste burning under UV light irradiation. Gas concentrations were detected by a gas chromatography thermal conductivity detector (GC-TCD) and gas chromatography-mass spectroscopy (GC-MS).

2. MATERIAL AND METHODS

2.1 Materials and Instruments

The titanium dioxide (TiO_2) (anatase-type) powder is produced by Sigma Aldrich. Cobalt nitrate powder ($Co(NO_3)_2$) was purchased from Nitra Kimia, Indonesia. UV lamp (220V, 50 Hz, 6W) was used as light sources. X-ray diffraction (Shimadzu XRD-6000) and diffuse reflectance UV-visible spectroscopy (Shimadzu UV-1700) were used to characterize the photocatalyst doped. Contaminated smoke is generated from burned waste such as plastic, paper, cardboard, and dry leaves. The 5-mL venoject tube was used to collect the smoke samples. Gas chromatography thermal conductivity detector (GC-TCD, Shimadzu GC 8A) and gas chromatography-mass spectroscopy (GC-MS, Shimadzu QP 2010 SE) were utilized to measure the concentration of the molecules of the samples.

2.2 Method and Procedure

The testing chamber in this study was constructed using a modified hexagonal prismatic glass container with a hole for smoke and a hole for sample collection. UV lamps were installed inside the chamber as UV light sources. A fan was installed in one of the holes to introduce smoke so that the smoke would be attracted and enter the chamber. An illustration of the photocatalyst fabrication process and the test chamber are shown in Fig. 1. In this study, the TiO_2 photocatalyst was doped with Co derived from $Co(NO_3)_2$. 40 mg of TiO_2 and 10 mg of $Co(NO_3)_2$ were dissolved in 5 mL of distilled water and stirred with a stirring speed of 570 rpm for 2 hours at room temperature to produce a homogenous photocatalyst solution. The solution was then sprayed on two sheets of mica (13 × 29 cm) coated with aluminum foil for photocatalyst test under UV light. These sheets aim to cover the glass in the test room so that UV light does not radiate out. After spraying on the mica, the solution was dried in a furnace at 90 °C for 1 hour. Then, the mica was mounted on the inner side of the test chamber.

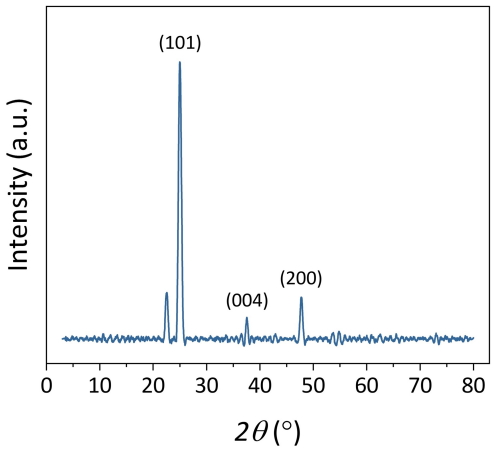

Figure 2. XRD pattern of $TiO_2/Co(NO_3)_2$ photocatalyst

The photocatalyst was synthesized in solid phase (powder) for material characterization and then tested using XRD

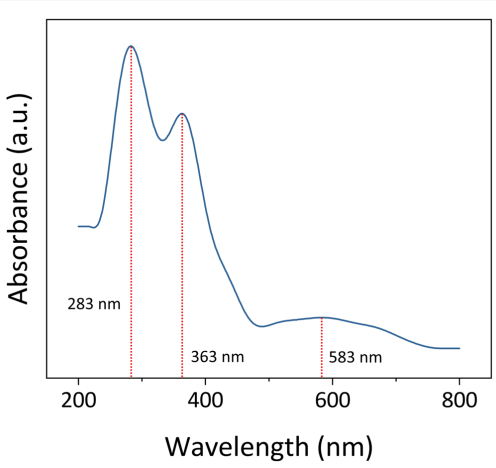

Figure 3. Absorbance spectrum of $TiO_2/Co(NO_3)_2$

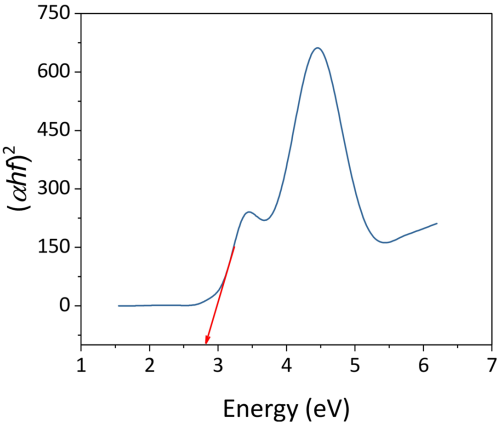

Figure 4. Tauc's plot on $TiO_2/Co(NO_3)_2$

to determine the type of crystal. Analysis was carried out with diffraction angles (2θ) in the range of 3°C–80°C and scanned continuously at a scan rate of 4 degrees·s^{-1}. XRD was conditioned at a voltage of 40 kV with a current of 30 mA. The resulting data are 2θ and intensity, then presented in a graph to determine the intensity peaks. The values calculated in XRD are crystallite size (t) and lattice parameters (a and c) with the following equations (Eq. 1 and Eq. 2).

$$t = \frac{K\lambda}{\beta \cos\theta} \tag{1}$$

$$\frac{1}{d^2} = \frac{h^2}{a^2} + \frac{k^2}{b^2} + \frac{l^2}{c^2} \tag{2}$$

where K is Scherrer constant (0.9), λ is X-ray wavelength (0.154 nm), β is the full width at half the maximum intensity of the reflection peak, θ is diffraction angle, d is the distance between Bragg planes, and (hkl) is miller index [16]. Photocatalysts synthesized in the solid phase (powder) are also tested using DR UV-vis spectroscopy to ensure photocatalyst band gap energy changes after doping with $Co(NO_3)_2$. Data acquisition is performed at a wavelength of 200–800 nm every 1 nm. The data results were then analyzed using Tauc's Plot method, which is the relationship between absorption coefficient (α) and incident photon energy hf in the form of (Eq. 3):

$$(\alpha hf)^{\frac{1}{m}} = c(hf - E_g) \tag{3}$$

where α is the absorbance coefficient used in the Tauc Plot method, h is the photon energy (eV), c is a constant, and Eg is the band gap energy. The value of m depends on the type of transition: m = 1/2 for direct and permitted transitions, m = 2 for indirect transitions, and m = 3/2 for forbidden transitions [22]. OriginLab software was used to determine the bandgap energy of the photocatalyst.

The photocatalyst test begins by filling the chamber to the brim with polluted smoke/gas by capturing the combustion exhaust using a funnel and hose connected to the vent hole in the chamber. The UV lamp is then turned on. Gas samples were taken with a syringe directly into a 5 mL venoject tube to preserve the gas. In the first test to observe the degradation of CO_2, samples were taken every 2 hours from before the reaction occurred (t = 0 s) to 6 hours. In the second test to observe the degradation of HCN and CH_4, samples were collected every 10 minutes from pre-reaction (t = 0 s) to 40 minutes.

Gas samples stored in venoject tubes were analyzed by GC-TCD and GC-MS to determine changes in the CO_2, HCN, and CH_4 concentrations after the photocatalyst test. The concentration of the molecules in the gas is indicated by the percentage of the area of the peaks on the graph produced by the detector. The percentage of CH_4 and CO_2 degradation is calculated using the following equation (see Eq. 4).

$$\text{Degradation}(\%) = \left(1 - \frac{C_t}{C_0}\right) \times 100\% \tag{4}$$

where Ct is the concentration of the molecule at time t, and C_0 is the initial concentration of the molecule [13]

3. RESULTS AND DISCUSSION

3.1 Crystral Size Analysis of $TiO_2/Co(NO_3)_2$ Photocatalyst

The crystal structure of the photocatalyst layer used in this study was analyzed using an X-ray diffractometer (XDR). The data obtained was further analyzed using OriginLab software to determine the diffraction peaks. The peaks are the scattering of light hitting the TiO_2/Co crystal, which interferes constructively. The XRD patterns of $TiO_2/Co(NO_3)_2$ photocatalyst is shown in Fig 2.

Based on Fig. 2, diffraction peaks indicate that X-rays hit the crystal plane. Four diffraction peaks are visible on the $TiO_2/Co(NO_3)_2$, namely at 2θ of 22.526°C, 25.013°C, 37.552°C, and 47.761°C. These diffraction peaks were compared with the TiO_2 standard diffractogram from the Joint Committee on Powder Diffraction Standards-International Center for Diffraction Data (JCPDS-ICDD) No. 21–1272. The first peak did not find its Miller index from these data, so further analysis could not be performed. Meanwhile, the Miller indices at 2θ of 25.013°C, 37.552°C, and 47.761°C are (101), (004), and (200), respectively. The results of this crystal field analysis indicate that the detected material is anatase-type TiO_2 [14, 15, 19]. The highest diffraction peak of the $TiO_2/Co(NO_3)_2$ photocatalyst is located at 2θ of 25.013°C with plane (101). The peak appears due to the effect of the addition of $Co(NO_3)_2$ on TiO_2, which then characterizes the material we produce. Through the calculations in Eq. 1 and Eq. 2, the values in Table 1 are obtained.

Based on the calculations performed, the crystallite size of the $TiO_2/Co(NO_3)_2$ is (15.38 ± 0.03) nm. The crystallite size is smaller than pure TiO_2, which is 19.82 nm [13]. Co

Table 1. Crystallite structure analysis results of $TiO_2/Co(NO_3)_2$

2θ (°)	FWHM (rad)	Miller Index (hkl)	Crystallite size (nm)	Lattice parameters (Å)	
				a	*c*
25.013	0.00923	-101	15.38 ± 0.03	3.8 ± 0.3	9.3 ± 0.3

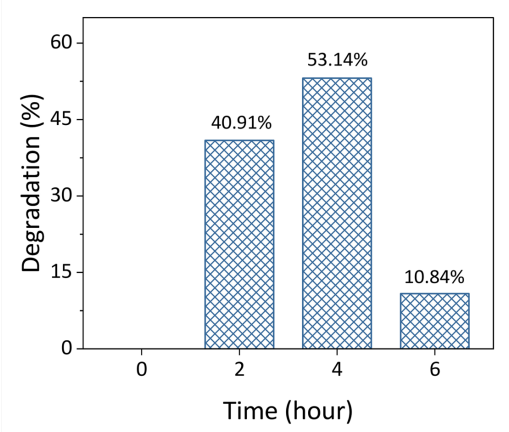

Figure 5. Percentage degradation of CO_2 pollutant of waste burning using $TiO_2/Co(NO_3)_2$ photocatalyst under UV light irradiation

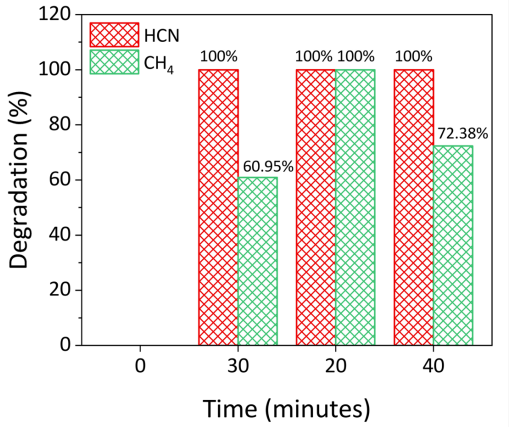

Figure 6. Percentage degradation of CH_4 and HCN pollutants from waste burning using $TiO_2/Co(NO_3)_2$ photocatalyst under UV irradiation

ions in the lattice seem to form a complex with oxygen on TiO_2, thus suppressing the growth of TiO_2 crystals [13]. This small crystallite size makes the surface of the material high, allowing the crystals to be evenly distributed. Meanwhile, the obtained lattice parameters (a and c) belong to anatase type TiO_2 [15]. Although the value is different, it is still within the calculation error range. Small differences from the calculation with the reference (a = 3.784 and c = 9.515 [15, 23]) result from the addition of $Co(NO_3)_2$ on TiO_2. This indicates that the doping used does not significantly change the crystal structure of TiO_2. Therefore, $Co(NO_3)_2$ doping does not inhibit the catalytic function of TiO_2.

3.2 Band Gap Energy of $TiO_2/Co(NO_3)_2$ Photocatalyst

The band gap energy of $TiO_2/Co(NO_3)_2$ photocatalyst was analyzed using DR UV-vis spectroscopy in a wavelength range of 200–800 nm. The increasing absorbance value indicates that the intensity of the absorbed light is becoming greater, resulting in many free electrons that will fill the conduction band and produce an electric current. The absorbance of TiO_2 and $TiO_2/Co(NO_3)_2$ is shown in Fig. 3.

From the absorbance spectra, it can be seen that the highest absorbance on $TiO_2/Co(NO_3)_2$ occurs when exposed to a wavelength of 283 nm, then drops and rises again at 363 nm, then drops dramatically and rises slowly to peak at 583 nm (see Fig. 3). When compared with the absorption spectrum of pure TiO_2 [24], there are differences in the wavelength of maximum absorption. In pure TiO_2, there is only one maximum absorbance peak at a wavelength of 302 nm [24]. The difference in absorbance spectra was believed to be an impact of the addition of $Co(NO_3)_2$ and affects the photocatalyst's ability to absorb light. The value of the band gap energy is very important because it affects the ability of the material to form electrons and holes. This energy determines how much photon energy is required to activate the photocatalytic process. The lower the band gap energy of a material, the lower the photon energy required to initiate photocatalysis. The band gap energy of the materials used in this study was calculated using Tauc's Plot method. The data obtained from the DR UV-vis spectroscopy was processed in OriginLab software to obtain a graph absorption coefficient $(\alpha hf)^2$ vs the photon energy (hf). Then, extrapolation was performed in the region of the curve that increased sharply, as shown in Fig 4.

The red line in Fig. 4 is an extrapolation line made using Tauc's plot method, which shows the material's band gap. The band gap energy of $TiO_2/Co(NO_3)_2$ was obtained from the extrapolation line, which is 2.81 eV. The anatase band gap energy of TiO_2, which was initially 3.2 eV [19], becomes smaller after adding $Co(NO_3)_2$. The reduction in band gap energy, attributed to the presence of Co as a transition metal, induces the formation of an impurity state between the conduction band and the valence band in TiO_2. As the band gap is smaller due to the incorporation of Co into the TiO_2 lattice, the absorption edge shifts towards longer wavelengths (redshift). In this investigation, to surpass the band gap energy of 2.81 eV, light with a wavelength of 441.52 nm was necessary to activate the photocatalyst.

3.3 The Mechanism Of Degradation Of CO_2 and CH_4 Air Pollutants with $TiO_2/Co(NO_3)_2$ Photocatalyst

The degradation process of air pollutants can be carried out by the photocatalytic process on $TiO_2/Co(NO_3)_2$. Photocatalyst materials typically exist in semiconductors, capable of initiating chemical reactions upon exposure to photon energy surpassing the band gap energy. Initially, TiO_2 has a band gap energy of 3.2 eV [19]. However, after adding $Co(NO_3)_2$, the band gap energy becomes 2.81 eV due to Co^{2+} replacing Ti^{4+} in the TiO_2 crystal structure. The size of Co^{2+} ions (radius 0.074 nm) is almost similar to Ti^{4+} (radius 0.068 nm), allowing them to enter the TiO_2 crystal to decrease the band gap and increase the activity of the photocatalyst [13].

Photons with energy greater than 2.81 eV, such as UV light, can cause electronic transitions from the valence band to the conduction band. Electrons in the O 2p orbitals in

Table 2. Results of GC-TCD analysis of the degradation of CO_2 under UV light irradiation

Time (hours)	Retention time (min)	Area (%)	Compound name	Degradation (%)
0	8.723	1.513	CO_2	0
2	8.719	0.894	CO_2	40.912
4	8.718	0.709	CO_2	53.139
6	8.746	1.349	CO_2	10.839

Table 3. Results of GC-MS Analysis of the degradation of HCN and CH_4 under UV light irradiation

Time (min)	Retention time (min)	Area (%)	Similarity Index	Compound name	Degradation (%)
0	2.211	1.18	50	HCN	0
	2.615	1.05	52	CH_4-D4	0
10	-	-	-	HCN	100
	2.031	0.41	51	CH_4	60.952
20	-	-	-	HCN	100
	-	-	-	CH_4	100
40	-	-	-	HCN	100
	0.25	0.29	47	CH_4	72.381

the valence band are excited to the Co 3d and Ti 3d orbitals in the minimum conduction band. The presence of valence band electrons creates holes (hvb^+) due to electron donors. Meanwhile, the conduction band produces electrons (ecb^-) as electron acceptors. This process is where the decomposition begins. The holes will interact with the water molecules in the air, while the electrons will interact with the oxygen in the air. The reaction of electrons and holes with oxygen and water produces hydroxyl radicals, which can break down organic polymers such as CH_4. On the other hand, CO_2 can be degraded due to adsorption by the photocatalyst layer but cannot be chemically decomposed. The chemical reaction that occurs is as follows [25].

$$Co(NO_3)_2 - TiO_2 + hf \rightarrow Co(NO_3)_2 - TiO_2(e^+_{cb} + h^-_{vb}) \quad (5)$$

$$h^+_{vb} + H_2O \rightarrow H^+ + HO^{\cdot}(\text{oxidation}) \quad (6)$$

$$e^+_{cb} + O_2 \rightarrow O_2^{\cdot -}(\text{reduction}) \quad (7)$$

$$O_2^{\cdot -} + H^+ \rightarrow HO_2^{\cdot} \quad (8)$$

$$HO_2^{\cdot} + HO_2^{\cdot} \rightarrow H_2O_2 + O_2 \quad (9)$$

$$H_2O_2 + e^+_{cb} \rightarrow HO^{\cdot} + OH^- \quad (10)$$

$$H_2O_2 + hv \rightarrow 2HO^{\cdot} \quad (11)$$

$$CH_4 + 4HO^{\cdot} + O_2 \rightarrow CO_2 + 4H_2O \quad (12)$$

3.4 Degradation Of Air Pollutants With Photocatalysts Under Ultraviolet Light Irradiation

The first energy source used is ultraviolet light ($\lambda < 400$ nm), which has energy greater than 2.81 eV, the bandgap energy of $TiO_2/Co(NO_3)_2$ photocatalyst. This energy can activate the photocatalytic process on the photocatalyst layer. In the first observation (i.e., degradation of CO_2), time variations of 0, 2, 4, and 6 hours were used (see Table 2). GC-TCD detected the concentration of the CO_2. The GC-TCD instrument can only make semi-quantitative measurements, which is the amount of molecular concentration expressed in the percentage range based on the compound's retention time. Retention time is the required time for the analyte to be injected until the detector captures the signal in the form of a peak plot generated by the instrument. The peaks of the graph have an area whose percentage represents the concentration of the compounds detected in the gas being analyzed. The degradation percentage is calculated using Eq. 4 based on these concentrations.

The calculation result shows increased CO_2 degradation at 2 and 4 hours (see Fig. 5). The increase in the degradation percentage with the irradiation time is caused by the number of electrons excited from the valence band to the conduction band to produce free electrons on the surface of the photocatalyst layer, which interacts with CO_2 in the air. The ability of the photocatalyst to degrade CO_2 pollutants reaches a maximum of 53.14% for 4 hours (see Table 2). However, the percentage decreased drastically to 10.84% at 6 hours, and there was a possibility of the photocatalyst experiencing saturation, so its degradation ability decreased. Saturation may occur because CO_2 previously adsorbed on the photocatalyst's surface blocks the photocatalytic process. Another possibility is that CO_2 is desorbed, increasing the measured concentration.

Furthermore, the degradation ability of the $TiO_2/Co(NO_3)_2$ photocatalyst under UV light irradiation was observed with time variations of 0, 10, 20, 30, and 40 minutes using GC-MS to observe the degradation of HCN and CH_4. Similar to GC-TCD, GC-MS can only make semiquantitative measurements by area percentage. GC-MS uses the similarity index (the degree of similarity of the detector data to the instrument's reference) to determine which molecules are detected in the peaks of the graph produced by the detector.

In the second observation (i.e., degradation of HCN and CH_4 under UV light), Table 3 shows no HCN and CH_4 molecules initially (t = 0 s). After the photocatalyst was activated with UV light energy, the HCN molecule no longer appeared during the observation. The phenomenon shows that the photocatalyst can degrade HCN within 10 minutes (see Fig. 6). Meanwhile, the CH_4 molecule experienced a degradation of 60.95% in the first 10 minutes and an increase in the percentage of degradation to 100% in the first 20 minutes. However,

the CH_4 molecule suddenly reappeared in 40 minutes with a degraded percentage of 72.38%. This phenomenon is possibly due to the photocatalyst experiencing saturation, which decreases the photocatalyst's ability to degrade.

4. CONCLUSION

The doping of $Co(NO_3)_2$ onto the TiO_2 photocatalyst was successfully carried out. The crystallite size of the photocatalyst after doping is (15.38 ± 0.03) nm, while the lattice parameters a and c are (3.8 ± 0.3) Å and (9.3 ± 0.3) Å, respectively. These results indicate that Co doping does not change the crystal structure of TiO_2, namely the anatase phase. Furthermore, the band gap energy decreased after doping to 2.81 eV, which UV light can easily transmit. As a result, the $TiO_2/Co(NO_3)_2$ photocatalyst successfully degraded CO_2 gas pollutants by 53.139% for 4 hours, HCN by 100% for 10 minutes, and CH_4 by 72.381% for 40 minutes under UV light irradiation.

ACKNOWLEDGMENTS

Kamila Munna acknowledges an undergraduate scholarship from the Ministry of Education, Culture, Research, and Technology of the Republic of Indonesia through the Bidikmisi program and a master scholarship from the Ministry of Finance through the Indonesian Endowment Fund for Education (LPDP). Rizky Aflaha acknowledges a Ph.D. scholarship from the Ministry of Education, Culture, Research, and Technology of the Republic of Indonesia through the PMDSU program. The authors thank Mr. Dhe, Eka Dwi Lestari, and Nurul Imani Istiqamah, who helped greatly in the Materials Physics Laboratory at Gadjah Mada University.

FUNDING

This work was funded by the Bantuan Pendanaan Perguruan Tinggi Negeri (BPPTN), Department of Physics Gadjah Mada University, under contract number 118/J01.1.28/PL.06.02/2020.

AUTHOR CONTRIBUTIONS

Kamila Munna: conceptualization; investigation; formal analysis; writing-original draft. **Rizky Aflaha:** visualization; validation; formal analysis; writing-review and editing. **Chotimah:** conceptualization; validation; funding acquisition; supervision. All authors approved the final manuscript.

REFERENCES

[1] J. J. Zhang, K. R. Smith, Indoor air pollution: a global health concern, British Medical Bulletin 68 (1) (2003) 209–225. https://doi.org/10.1093/bmb/ldg029.

[2] C.-C. Lin, C.-C. Chiu, P.-Y. Lee, K.-J. Chen, C.-X. He, S.-K. Hsu, K.-C. Cheng, The Adverse Effects of Air Pollution on the Eye: A Review, International Journal of Environmental Research and Public Health 19 (3) (2022) 1186. https://doi.org/10.3390/ijerph19031186.

[3] J. Girman, M. Apte, G. Traynor, J. Allen, C. Hollowell, Pollutant emission rates from indoor combustion appliances and sidestream cigarette smoke, Environment International 8 (1-6) (1982) 213–221. https://doi.org/10.1016/0160-4120(82)90030-7.

[4] C. Granier, C. Liousse, B. McDonald, P. Middleton, Anthropogenic Emissions Inventories of Air Pollutants, in: H. Akimoto, H. Tanimoto (Eds.), Handbook of Air Quality and Climate Change, Springer Nature Singapore, Singapore, 2023, pp. 3–52. https://doi.org/10.1007/978-981-15-2760-9_5. URL https://link.springer.com/10.1007/978-981-15-2760-9_5

[5] W. Gumtorntip, N. Kasitanon, W. Louthrenoo, N. Chattipakorn, S. C. Chattipakorn, Potential roles of air pollutants on the induction and aggravation of rheumatoid arthritis: From cell to bedside studies, Environmental Pollution 334 (2023) 122181. https://doi.org/10.1016/j.envpol.2023.122181.

[6] V. V. Tran, D. Park, Y.-C. Lee, Indoor Air Pollution, Related Human Diseases, and Recent Trends in the Control and Improvement of Indoor Air Quality, International Journal of Environmental Research and Public Health 17 (8) (2020) 2927. https://doi.org/10.3390/ijerph17082927.

[7] F. He, W. Jeon, W. Choi, Photocatalytic air purification mimicking the self-cleaning process of the atmosphere, Nature Communications 12 (1) (2021) 2528. https://doi.org/10.1038/s41467-021-22839-0.

[8] I. P. A. Kristyawan, A. Indra, I. G. A. Suradharmika, G. Setiaji, N. C. Putri, I. W. Oka, The effect of adding photocatalyst ceramics on reducing particulate matter in indoor air purification systems, IOP Conference Series: Earth and Environmental Science 1108 (1) (2022) 012008. https://doi.org/10.1088/1755-1315/1108/1/012008.

[9] R. Chen, J. Li, H. Wang, P. Chen, X. Dong, Y. Sun, Y. Zhou, F. Dong, Photocatalytic reaction mechanisms at a gas–solid interface for typical air pollutant decomposition, Journal of Materials Chemistry A 9 (36) (2021) 20184–20210. https://doi.org/10.1039/D1TA03705F.

[10] I. Ahmad, Y. Zou, J. Yan, Y. Liu, S. Shukrullah, M. Y. Naz, H. Hussain, W. Q. Khan, N. Khalid, Semiconductor photocatalysts: A critical review highlighting the various strategies to boost the photocatalytic performances for diverse applications, Advances in Colloid and Interface Science 311 (2023) 102830. https://doi.org/10.1016/j.cis.2022.102830.

[11] S. J. Armaković, M. M. Savanović, S. Armaković, Titanium Dioxide as the Most Used Photocatalyst for Water Purification: An Overview, Catalysts 13 (1) (2022) 26. https://doi.org/10.3390/catal13010026.

[12] C. B. Anucha, I. Altin, E. Bacaksiz, V. N. Stathopoulos, Titanium dioxide (TiO2)-based photocatalyst materials activity enhancement for contaminants of emerging concern (CECs) degradation: In the light of modification strategies, Chemical Engineering Journal Advances 10 (2022) 100262. https://doi.org/10.1016/j.ceja.2022.100262.

[13] S. N. Hoseini, A. K. Pirzaman, M. A. Aroon, A. E. Pirbazari, Photocatalytic degradation of 2,4-dichlorophenol by Co-doped TiO 2 (Co/TiO 2) nanoparticles and Co/TiO 2 containing mixed matrix membranes, Journal of Water Process Engineering 17 (2017) 124–134. https://doi.org/10.1016/j.jwpe.2017.02.015.

[14] L. Lu, C.-L. Zhang, S.-B. Mi, Probing interface structure and cation segregation in (In, Nb) co-doped TiO2 thin films, Materials Characterization 191 (2022) 112164. https://doi.org/10.1016/j.matchar.2022.112164.

[15] R. Singh, S. Dutta, A review on H2 production through photocatalytic reactions using TiO2/TiO2-assisted catalysts, Fuel 220 (2018) 607–620. https://doi.org/10.1016/j.fuel.2018.02.068.

[16] D. Komaraiah, E. Radha, J. Sivakumar, M. Ramana Reddy, R. Sayanna, Photoluminescence and photocatalytic activity of spin coated Ag+ doped anatase TiO2 thin films, Optical Materials 108 (2020) 110401. https://doi.org/10.1016/j.optmat.2020.110401.

[17] M. R. D. Khaki, M. S. Shafeeyan, A. A. A. Raman, W. M. A. W. Daud, Application of doped photocatalysts for organic pollutant degradation - A review, Journal of Environmental Management 198 (2017) 78–94. https://doi.org/10.1016/j.jenvman.2017.04.099.

[18] H. Lee, Y.-K. Park, S.-J. Kim, B.-H. Kim, S.-C. Jung, Titanium dioxide modification with cobalt oxide nanoparticles for photocatalysis, Journal of Industrial and Engineering Chemistry 32 (2015) 259–263. https://doi.org/10.1016/j.jiec.2015.08.025.

[19] S. Na-Phattalung, D. J. Harding, P. Pattanasattayavong, H. Kim,

J. Lee, D.-W. Hwang, T. D. Chung, J. Yu, Band gap narrowing of TiO2 nanoparticles: A passivated Co-doping approach for enhanced photocatalytic activity, Journal of Physics and Chemistry of Solids 162 (2022) 110503. https://doi.org/10.1016/j.jpcs.2021.110503.

[20] H. Liu, B. Lin, L. He, H. Qu, P. Sun, B. Gao, Y. Chen, Mesoporous cobalt-intercalated layered tetratitanate for efficient visible-light photocatalysis, Chemical Engineering Journal 215-216 (2013) 396–403. https://doi.org/10.1016/j.cej.2012.11.039.

[21] A. H. Mamaghani, F. Haghighat, C.-S. Lee, Hydrothermal/solvothermal synthesis and treatment of TiO2 for photocatalytic degradation of air pollutants: Preparation, characterization, properties, and performance, Chemosphere 219 (2019) 804–825. https://doi.org/10.1016/j.chemosphere.2018.12.029.

[22] O. R. Fonseca-Cervantes, A. Pérez-Larios, V. H. Romero Arellano, B. Sulbaran-Rangel, C. A. Guzmán González, Effects in Band Gap for Photocatalysis in TiO2 Support by Adding Gold and Ruthenium, Processes 8 (9) (2020) 1032. https://doi.org/10.3390/pr8091032.

[23] S. M. Gupta, M. Tripathi, A review of TiO2 nanoparticles, Chinese Science Bulletin 56 (16) (2011) 1639–1657. https://doi.org/10.1007/s11434-011-4476-1.

[24] G. R. Kandregula, K. V. Rao, A. Chinthakuntla, V. Rajendar, Green Synthesis of TiO2 Nanoparticles Using Hibiscus Flower Extract.

[25] Nasikhudin, M. Diantoro, A. Kusumaatmaja, K. Triyana, Study on Photocatalytic Properties of TiO $_2$ Nanoparticle in various pH condition, Journal of Physics: Conference Series 1011 (2018) 012069. https://doi.org/10.1088/1742-6596/1011/1/012069.

